PH4201: Advanced Optics Laboratory

Fabry-Perot Interferometer

Susnata Chattopadhyay*†
22MS077

Indian Institute of Science Education and Research (IISER) Kolkata,
Mohanpur, West Bengal, 741246, India.

June 6, 2026

Abstract

In this experiment we study the Fabri-Perot Interferometer to find the spacing between the mirrors in the etalon, which will be used to find the unknown wavelength of the given laser. In the second part of the experiment we will find the finesse (resolution) of the Interferometer by various image analysis techniques and also by experimental determination of reflectivity.

Contents

1 Theory **2**
1.1 Condition for Multiple-Beam Interference . . . 2
1.2 Fabry Perot Interferometer . . . 2
1.3 Formation of Circular Fringes . . . 3

2 Working Formula **3**
2.1 Theoretical Determination of Plate Separation . . . 3
2.2 How is the interference happening? . . . 4

3 Experimental Setup **5**

4 Data Analysis **5**
4.1 Determining the etalon spacing - d . . . 5
4.2 Determination of unknown wavelength (*green laser*) . . . 6
4.3 Determination of Free Spectral Range (FSR) of our setup . . . 7
4.4 Determination of Finesse by Airy function fit . . . 7
4.5 Determination of Finesse by Lorentzian Peak fits . . . 9
4.6 Determination of Finesse by Contrast . . . 10
4.7 Determination of Reflectivity Finesse . . . 10

5 Discussion **12**
5.1 Sources of Error . . . 12

6 Conclusion **12**

*www.susnata.com †sc22ms077@iiserkol.ac.in

1 Theory

1.1 Condition for Multiple-Beam Interference

Consider monochromatic light of wavelength λ incident on the interferometer at an angle θ with respect to the normal. Constructive interference occurs when the phase difference between successive transmitted beams is an integer multiple of 2π. This condition leads to

$$2d\cos\theta = m\lambda, \tag{1}$$

where m is the interference order, an integer. Each allowed value of m corresponds to a transmission maximum of the interferometer.

For normal incidence ($\theta = 0$), the condition simplifies to

$$2d = m\lambda. \tag{2}$$

Thus, only discrete wavelengths are transmitted for a given plate separation. We can use the radius of different order of fringes to calculate the etalon spacing (d).

1.2 Fabry Perot Interferometer

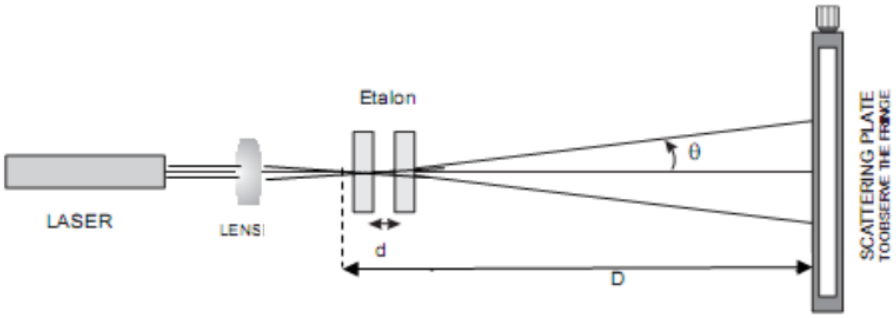


Figure 1: The schematic diagram of our setup. The distance d is the unknown air spacing between the etalon that we aim to calculate in this experiment, while D is the distance between the screen and the focus of the lens (in this case coinciding with the etalon itself).

The Fabry–Perot interferometer is an optical instrument that operates on the principle of multiple-beam interference produced between two parallel, partially reflective surfaces. Developed by Charles Fabry and Alfred Perot as an advancement over conventional two-beam interferometers, it enables exceptionally high spectral resolution. In contrast to Michelson-type interferometers, the Fabry–Perot configuration makes use of repeated internal reflections, which gives sharper interference fringes and significantly improve resolving power.

Fabry Perot Interferometer essentially consists of two glass or quartz plates with plane surfaces. The inner surfaces are coated with partially transparent films of high reflectivity, and are *nearly* parallel. The plates themselves are made slightly *prismatic*[1], in order to avoid disturbing effects due to reflections at the outer uncoated surfaces. The plates are separated by a fixed spacer d (or L), which is commonly a hollow cylinder of invar or silica with three projecting studs at each end, and the plates are kept in place by the pressure of springs. The spacer is optically worked so that the planes defined by the studs are as nearly parallel as possible, and fine adjustments can be made by varying the spring pressure. This form of the interferometer, with fixed plate separation, is called a **Fabry–Perot etalon**.

[1] prismatic plates are used to suppress unwanted multiple reflections by slightly tilting the surfaces so that spurious reflections are deflected out of the optical path and do not overlap with the main interference beams. This ensures that only the desired multiple-beam interference between the two parallel mirrors contributes to the observed fringes.

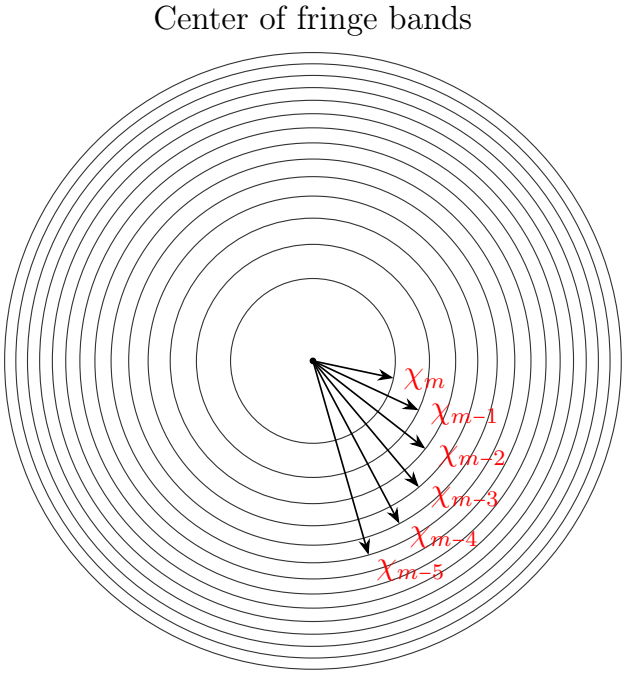
1.3 Formation of Circular Fringes

In practical experiments, the incident laser beam is slightly divergent. Different rays enter the interferometer at different angles θ, leading to transmission maxima at different radial positions on a screen. As a result, a system of concentric circular fringes is observed. One particular cone of light after multiple reflection within the two mirrors generate one ring (bright or dark). More such divergent cones of light generate the overall interference pattern.

The central bright fringe corresponds to the highest interference order, while the order decreases with increasing fringe radius. For small angles, the angular dependence can be related to the fringe radius, allowing quantitative analysis of the pattern.

2 Working Formula

2.1 Theoretical Determination of Plate Separation



Line drawing of Fabrey Perot fringe pattern

From the interference condition for a Fabry-Perot etalon,

$$m\lambda = 2d\cos\theta_m, \tag{3}$$

where d is the separation between the plates and θ_m is the angle corresponding to the m^{th} circular fringe. **As the angle θ increases, the order m decreases and hence the fringe radius increases.**

For successive rings (farther out),

$$\begin{aligned}(m-1)\lambda &= 2d\cos\theta_{m+1},\\ (m-2)\lambda &= 2d\cos\theta_{m+2},\\ &\vdots\\ (m-n)\lambda &= 2d\cos\theta_{m+n}.\end{aligned}$$

Subtracting the first equation from the last,

$$n\lambda = 2d\left(\cos\theta_m - \cos\theta_{m+n}\right). \tag{4}$$

For small angles, which is valid for Fabry-Perot fringes,

$$\tan\theta_m \approx \theta_m = \frac{\chi_m}{D}, \tag{5}$$

where χ_m is the radius of the m^{th} fringe and D is the distance between the etalon (more specifically the focus of the converging lens) and the screen.

Hence,

$$\cos\theta_m \approx 1 - \frac{\chi_m^2}{2D^2}. \tag{6}$$

Substituting this approximation in Eq. 4, we obtain,

$$n = \frac{d}{D^2\lambda}\left(\chi_{m+n}^2 - \chi_m^2\right) \implies \boxed{\chi_n^2 = \left(\frac{D^2\lambda}{d}\right)n} \tag{7}$$

Thus, a plot of fringe order difference $(\chi_{m+n}^2 - \chi_m^2) \equiv \chi_n^2$ versus n gives a straight line. From the slope of this graph, the separation d between the plates of the Fabry Perot etalon can be calculated using

$$d = \frac{D^2\lambda}{\text{slope}}. \tag{8}$$

or equivalently, an unknown wavelength can be calculated as

$$\lambda_? = \frac{(\text{slope})\text{d}}{D^2} \tag{9}$$

2.2 How is the interference happening?

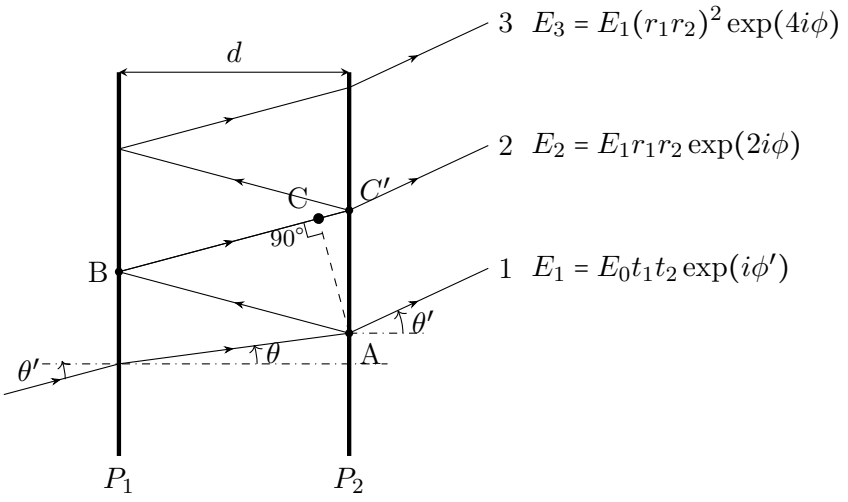


Figure 2: Multiple beam interference in Fabry-Perot interferometer

The phenomenon at its core is based on the transmission of light incident at two parallel beam splitters/surfaces P_1 and P_2, as depicted in Fig. 2

The sum of electric fields of the incident beam and its successive reflections is given by

$$E_t = E_0tt'e^{ik\Delta}\left[1 + r^2e^{i2k\Delta} + r^4e^{i4k\Delta} + \cdots + r^{2n}e^{i2nk\Delta} + \cdots\right] = \frac{E_0tt'e^{ik\Delta}}{1 - r^2e^{i2k\Delta}}, \tag{10}$$

where Δ is the phase of the first transmitted wave. Now the intensity distribution can be written as

$$I_t = \left(\frac{1}{2}\epsilon_0c\right)E_tE_t^*, \tag{11}$$

$$= I_0\frac{|tt'|^2}{(1-r^2)^2 + 4r^2\sin^2(k\Delta/2)} \tag{12}$$

Using the conditions $r = -r'$ and $r^2 + tt' = 1$ in the above equations, we end up with

$$I_t = I_0 \frac{(1-r^2)^2}{(1-r^2)^2 + 4r^2 \sin^2(k\Delta/2)} \tag{13}$$

Rewriting this, we get

$$\boxed{T = \frac{\tau_0}{1 + (4\mathcal{F}^2/\pi^2)\sin^2(2\pi d/\lambda)}}, \tag{14}$$

where T is the transmission coefficient, τ_0 is the maximum possible transmission, $\mathcal{F}$ is the finesse, d is the spacing of the etalon, and λ is the wavelength of light.

3 Experimental Setup



Figure 3: The setup at the laboratory

Our experimental setup (see Fig. 3 and 1) comprises a *Fabry-Perot interferometer* (with notable adjustable mirror spacing, unlike a fixed-gap etalon), a focusing lens, two monochromatic gaussian beam sources (lasers), a study lamp, and a viewing screen for observing interference patterns. To quantify the diameter of various fringe orders, the screen is equipped with a needle mounted on a micrometer screw gauge.

4 Data Analysis

4.1 Determining the etalon spacing - d

The experimental values of $(\chi^2_{m+n} - \chi^2_m) \equiv \chi^2_n$ versus n are attached in Table 1 of the Appendix. The best fit plot is shown in Fig. 4

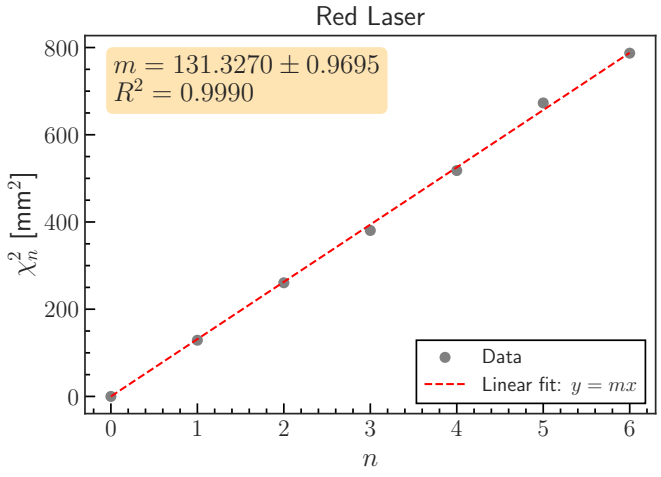


Figure 4: Performing the linear fit in a plot between the square of fringe radius ($\chi^2_n = \chi^2_{m+n} - \chi^2_m$) and fringe order ($n$) for the red laser. The corresponding best fit slope value and R^2 of the fit is quoted in the yellow box

The slope is obtained as

$$(\text{slope}) = 131.3270 \pm 0.9695 \text{ mm}^2$$

Now substitute the values of $D = 570$ mm, wavelength of red laser $\lambda = 655$ nm, and the slope in Eq. 8
We obtain the etalon spacing as

$$\boxed{d = 1.6204 \text{ mm}}$$

Error Analysis The maximum possible error associated with d is calculated as follows:

$$d = \frac{D^2 \lambda_R}{\text{slope}}$$

Since, $\lambda_R = 655$ nm is given to us, we consider $\Delta\lambda_R = 0$

$$\therefore \left|\frac{\Delta d}{d}\right| \leq \left|\frac{\Delta(\text{slope})}{(\text{slope})}\right| + 2\left|\frac{\Delta D}{D}\right|$$
$$\implies \left|\frac{\Delta d}{d}\right| \leq \frac{0.9695}{131.3270} + 2 \times \frac{1}{570}$$
$$\implies \left|\frac{\Delta d}{d}\right| \leq 0.0109$$
$$\implies |\Delta d| \leq 0.0176$$

Therefore,

$$\boxed{d = 1.6204 \pm 0.0176 \text{ mm}}$$

4.2 Determination of unknown wavelength (*green laser*)

Similarly, we plot $(\chi^2_{m+n} - \chi^2_m) \equiv \chi^2_n$ versus n (data in Table 2 in Appendix) and perform a slope fit (as shown in Fig. 5).

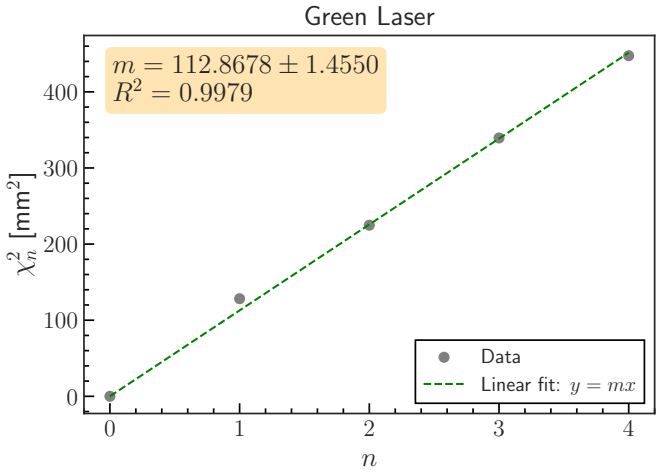


Figure 5: Performing the linear fit in a plot between the square of fringe radius ($\chi^2_n = \chi^2_{m+n} - \chi^2_m$) and fringe order ($n$) for the green laser. The corresponding best fit slope value and R^2 of the fit is quoted in the yellow box

The slope is obtained as

$$(\text{slope}) = 112.8678 \pm 1.4550 \text{ mm}^2$$

Now substitute the values of $D = 570$ mm, etalon spacing $d = 1.6204$ mm, and the slope in Eq. 9. We obtain the wavelength of green laser as-

$$\boxed{\lambda = 562.9147 \text{ nm}}$$

Error Analysis The maximum possible error associated with λ_G is calculated as:

$$\lambda_G = \frac{d \times (\text{slope})}{D^2}$$

$$\begin{aligned}
\therefore \left|\frac{\Delta\lambda_G}{\lambda_G}\right| &\leq \left|\frac{\Delta(\text{slope})}{(\text{slope})}\right| + 2\left|\frac{\Delta D}{D}\right| + \left|\frac{\Delta d}{d}\right| \\
&\leq \frac{1.455}{112.868} + 2 \times \frac{1}{570} + \frac{0.0176}{1.6204} \\
&= 0.0273 \\
\implies |\Delta\lambda_G| &\leq 15.3457
\end{aligned}$$

Therefore,

$$\boxed{\lambda_G = 562.9147 \pm 15.3457 \text{ nm}}$$

4.3 Determination of Free Spectral Range (FSR) of our setup

FSR is the spacing in frequency (or wavelength) between two successive transmission peaks of the interferometer. The free spectral range (FSR) is defined as:

$$\Delta\nu = \frac{c}{2d}, \tag{15}$$

where c is the speed of light and d is the etalon spacing.
Plugging in the values of c and d, we get FSR:

$$\boxed{\Delta\nu = 9.26 \times 10^{10} \text{ Hz} \approx 10^{11} \text{ Hz}}$$

FSR sets the maximum spectral range we can observe without ambiguity. If two spectral lines are separated by more than the FSR, they can overlap into adjacent orders and become indistinguishable. In practice, we can only uniquely measure frequencies within one FSR. Beyond that, the pattern repeats.

Error Analysis The maximum possible error associated with FSR is calculated as:

$$\Delta\nu = \frac{c}{2d}$$

So,

$$\left|\frac{\delta(\Delta\nu)}{\Delta\nu}\right| \leq \left|\frac{\Delta d}{d}\right| = 1.09\%$$

4.4 Determination of Finesse by Airy function fit

The **finesse** is a number which characterizes the width/ sharpness of the fringes (maxima). It should be noted, that Finesse only serves as an indicator, and various definitions to quantify it may NOT be mathematically equivalent. However, they must atleast lie in the same order of magnitude.

After placing the converging lens to the other side of the etalon, we find the fringes to change from *circular* to *linear*. We proceed to take a snapshot of the same through our smartphones by suitable adjustments of exposure and ISO. Upon imaging the fringe (Fig. 6), we then extract it's line profile with the help of a software (ImageJ) and begin our analysis.

Firstly, we calibrate X-axis from `pixel_numbers` to physical scale in milli-meters. This is done by manually measuring the width of the 3rd bright fringe from the left with a ruler and then scale the X-axis with respect to it. Then we measure the maximum transmittance (τ_{exp}) of our interferometer setup with the help of a light powermeter. We then rescale (or normalise) the Y-axis such that the tip of highest peak corresponds to τ_{exp}. Thus, our Y-axis represents the Transmissivity (T) of the fringe pattern (see Fig. 7).

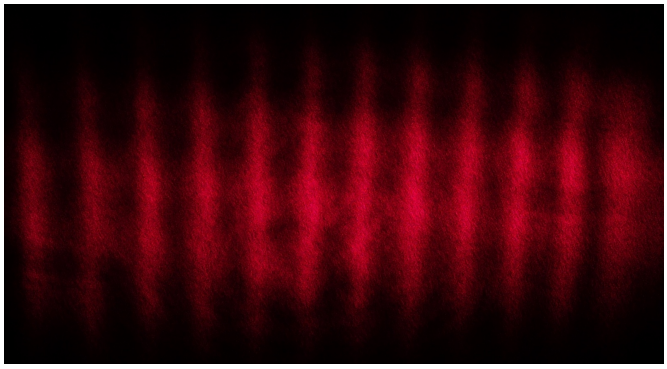


Figure 6: The image of linear fringe that we used in our analysis

$$\tau_{\text{exp}} = \frac{\text{Transmitted Power (mW)}}{\text{Incident Power (mW)}} = 1 - \frac{\text{Reflected Power (mW)}}{\text{Incident Power (mW)}} = 1 - \frac{16.4}{47.6} \simeq 0.655$$

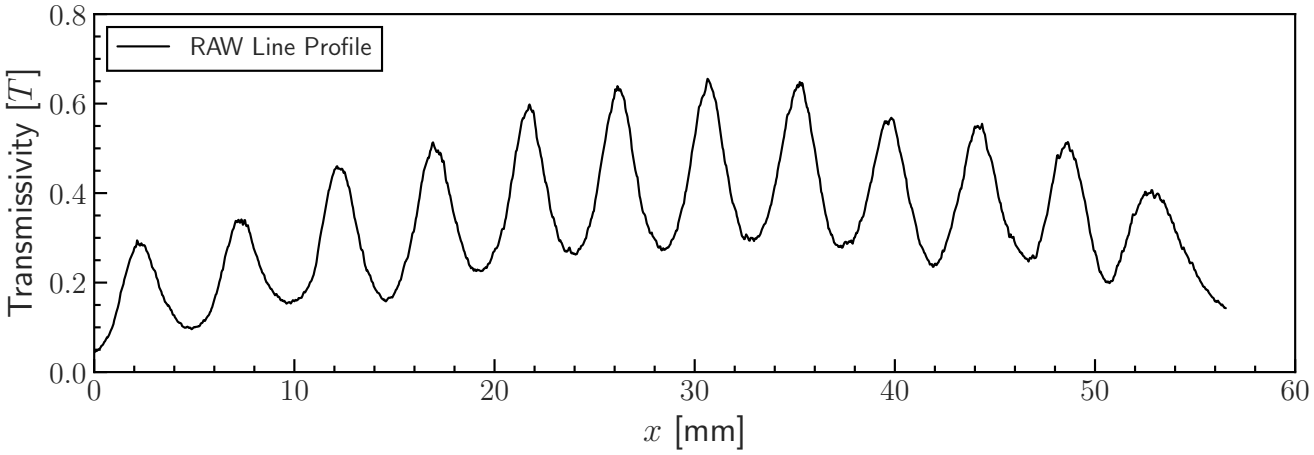


Figure 7: Extracted line profile of the fringe in Fig. 6

Next, since our laser is a *gaussian beam*, we need to subtract a gaussian profile (Fig. 8) with an offset[2] $[f(x|\mu_0, \sigma_0^2, A_0, H_0) = H_0 + A_0 \times \mathcal{N}(\mu_0, \sigma_0^2)]$, to bring all the peaks to the same level. We add the vertical offset (that was obtained after fitting) to the line profile, to get the beam shape corrected line profile [3] in Fig. 9, on which we fitted the Airy function (Eq. 16).

$$\boxed{T(x|y_0, \tau_{\text{calc}}, \mathcal{F}, a, b) = y_0 + \frac{\tau_{\text{calc}}}{1 + (\frac{2\mathcal{F}}{\pi} \sin(ax + b))^2}} \tag{16}$$

Here x corresponds to the real physical distance on the screen. It may be also be sometimes written as,

$$\boxed{T(x|y_0, \tau_{\text{calc}}, \mathcal{F}, a, b) = y_0 + \frac{\tau_{\text{calc}}}{1 + (\frac{2\mathcal{F}}{\pi} \sin\left(\frac{2\pi}{\lambda}(a\Delta L + b)\right))^2}} \tag{17}$$

But here, ΔL (or variation in spacing due to tilt between the two mirrors, as we go across the fringe) is the independent variable. The free spectral range (FSR) is basically the distance between 2 successive peaks. In ϕ-space, two successive peaks correspond to a phase difference of 2π. This implies in ΔL-space it corresponds to a separation of λ (since $\Delta\phi = (2\pi/\lambda)\Delta L$).

$$\Delta\phi = 2\pi \iff \Delta L = \lambda$$

Note: A great and wise choice of initial values matters a lot for a successful convergence!
After a successful fitting we obtain the value of **finesse** as

$$\boxed{\mathcal{F}_{\text{Airy}} = 1.6367 \pm 0.0188}$$

The best fit values of other parameters are quoted in Fig. 9

[2] to retain the background! [3] i.e. T[in Fig 8] - $A_0 \times \mathcal{N}(\mu_0, \sigma_0^2)$ = T[in Fig 9]

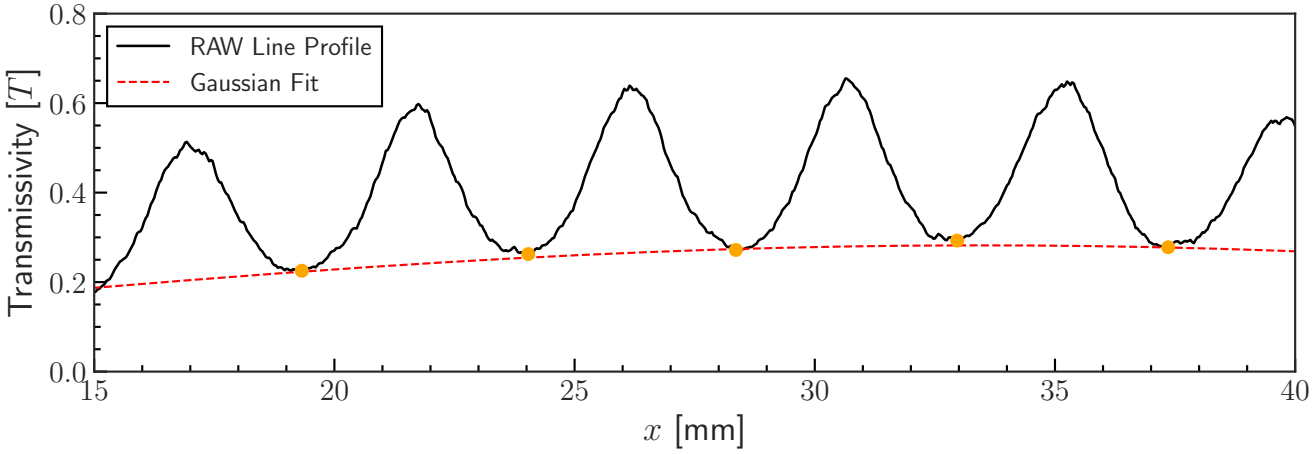


Figure 8: Gaussian Profile fitting of Fig. 7

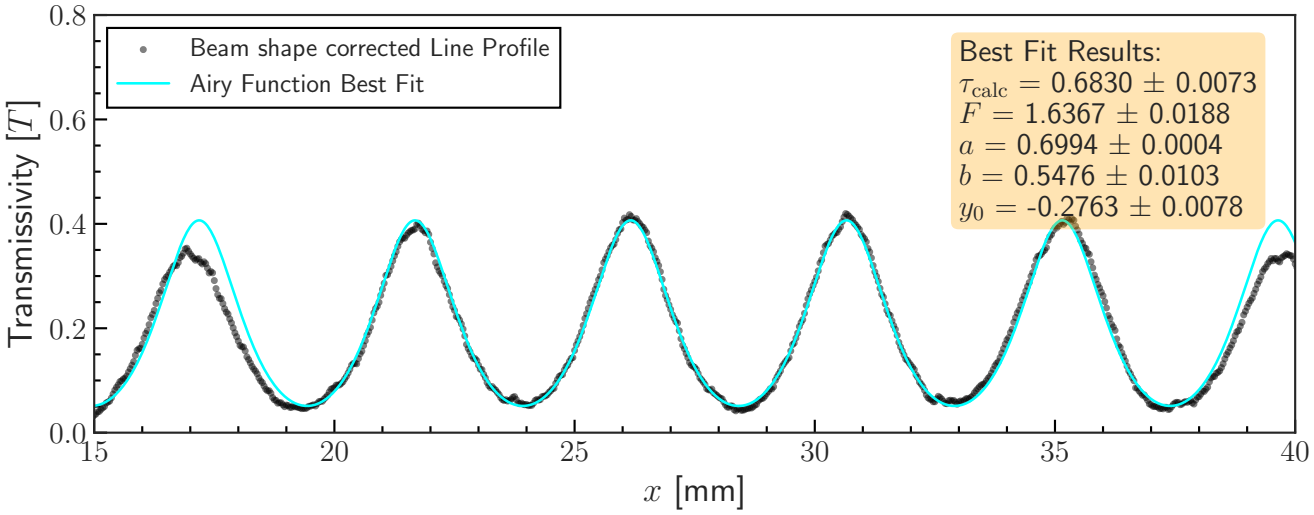


Figure 9: Fitting the Airy function (Eq. 16) in the beam shape corrected profile

4.5 Determination of Finesse by Lorentzian Peak fits

Observe the central 3 peaks in Fig. 9. As instructed in the manual, we fit them with Eq. (18) (a sum of 3 lorentzians with an offset) to determine the peak positions (10). But, note that all of them must have the same FWHM, because all maximas must be identical (ideally).

$$f(x|H_0, \sigma_{\text{FWHM}}, \vec{A}, \vec{x_c}) = H_0 + \sum_{i=1}^{3} A_i \frac{(\sigma_{\text{FWHM}}/2)^2}{(x - x_{c,i})^2 + (\sigma_{\text{FWHM}}/2)^2} \tag{18}$$

Recall, the sharpness of the fringes is conveniently measured by their half-intensity width, or half-width, which, in the case of the pattern in transmitted light, is the width between the points on either side of a maximum where the intensity has fallen to half its maximum value. In this case, the ratio of the separation of adjacent fringes and the half-width is known as **finesse** $\mathcal{F}$ of the fringes.

$$\mathcal{F} = \frac{\Delta(\text{peaks})}{\sigma_{\text{FWHM}}}$$

Since we have 3 peaks, we take the average separation between them, which is roughly 4.5453

$$\mathcal{F} = \frac{4.5453}{1.88288} \simeq 2.4140$$

Error Analysis The maximum possible error associated with finesse value is

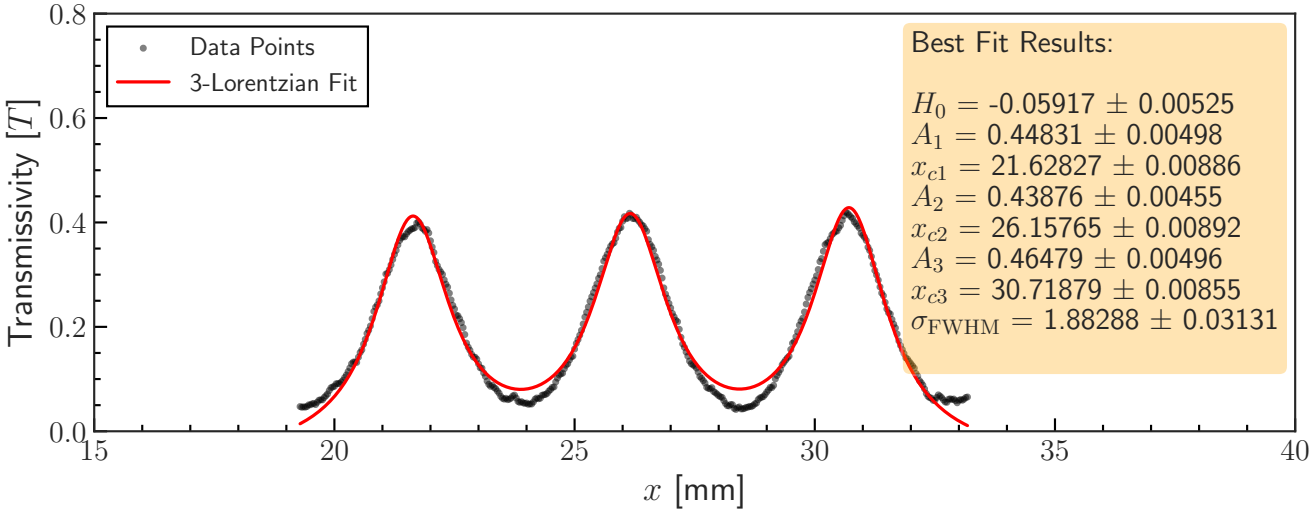


Figure 10: Lorentzian fit of the three central prominent peaks to determine the FWHM and peak positions

$$\left|\frac{\Delta\mathcal{F}}{\mathcal{F}}\right| \leq \frac{\delta[\Delta(\text{peaks})]}{[\Delta(\text{peaks})]} + \frac{\delta[\sigma_{\text{FWHM}}]}{[\sigma_{\text{FWHM}}]}$$
$$\leq \frac{0.00892}{4.5453} + \frac{0.03131}{1.88288} = 0.0186$$

Therefore,

$$\boxed{\mathcal{F} = 2.4140 \pm 0.0449}$$

4.6 Determination of Finesse by Contrast

To rate the suppression between maxima, the **Contrast** is defined as ratio of peak height to the minimum intensity. As calculated from corrected data in Fig. 9.

$$C = \frac{I_{\text{max}}}{I_{\text{min}}} = 10.0323$$

Contrast Finesse is defined as,

$$\mathcal{F}_C = \frac{\pi\sqrt{C-1}}{2} \simeq 4.7208$$

Error Analysis The readings were taken after imaging it through a smartphone camera. Associated errors include electronic noise, errors due to exposure adjustments, and possible projection effects on the screen.

4.7 Determination of Reflectivity Finesse

The reflectivity finesse is defined as

$$\mathcal{F}_{\text{R}} = \frac{\pi\sqrt{R}}{1-R}$$

Notice, as the reflectivity approaches unity, the finesse becomes very high. For high reflectivity, the transmission maxima are narrow, so the transmission of maxima of slightly different wavelengths can be easily distinguished. Because of this capability, the Fabry-Perot interferometer can also be used as a high resolution spectrometer.

As measured earlier with powermeter, we report the reflectivity value of the etalon setup as $R = \frac{16.4}{47.6} = 0.344$ (with Red laser). Therefore

$$\mathcal{F}_{\text{R}} = \frac{\pi\sqrt{0.344}}{1-0.344} \simeq 2.8074$$

Error Analysis

$$\mathcal{F}_R = \frac{\pi\sqrt{R}}{1-R}$$
$$\therefore \left|\frac{\Delta\mathcal{F}_R}{\mathcal{F}_R}\right| \leq \frac{1}{2}\left|\frac{\Delta R}{R}\right| + \left|\frac{\Delta R}{1-R}\right|$$

Error in R (least count of powermeter $= 0.1$ mW) :

$$\left|\frac{\Delta R}{R}\right| \leq \frac{0.1}{16.4} + \frac{0.1}{47.6} = 0.82\%$$
$$\implies |\Delta R| \leq 2.825 \times 10^{-3}$$

So,

$$\left|\frac{\Delta\mathcal{F}_R}{\mathcal{F}_R}\right| \leq \frac{0.8198}{2} \times 10^{-3} + \frac{2.825 \times 10^{-3}}{0.655} \implies |\Delta\mathcal{F}_R| \leq 0.0136$$

Hence,

$$\boxed{\mathcal{F}_R = 2.8074 \pm 0.0136}$$

5 Discussion

Projection effects in photographing linear fringes

When the linear Fabry–Perot fringes are projected onto a screen and imaged using a smartphone camera, projection geometry plays a significant role in distorting the observed pattern. As the camera sensor was not perfectly parallel to the screen, perspective effects caused fringes closer to the camera to appear more evenly spaced than those farther away. This geometric projection effect led to unequal apparent fringe spacing across the image. Lens aberrations and vignetting further modulate intensity across the field, led to unequal peak heights in the extracted line profile. Together, these projection and imaging effects introduce systematic distortions that must be corrected or carefully accounted for when analyzing finesse from photographed data.

Multiple fringe systems

Multiple circular fringe systems were observed that were not concentric. Again there were also diagonal linear fringes apart from the prominent one that was observed in the second part of the experiment. These might be caused by multiple reflections of the fringe pattern, due to imperfect curvature (or polishing) of the lens (or mirrors).

5.1 Sources of Error

Some of the possible sources of error in our experiment might be

- **Unclean Optical Surfaces:** Oil stain, grease or dust on the lenses/mirrors affect the quality of fringes (also reflectivity!).
- **Error in measuring diameter of higher order fringes:** As we moved farther from the central bright maxima, the circular fringes become closer and closer. This has resulted in a significant uncertainty in resolving the boundary of the circular fringes while taking measurements.
- **Imperfect Collimation:** The laser beam was not perfectly cylindrical, instead it was tapered along one of the axis (beam cross-section was elliptical). This might have affected the contrast of the fringes.
- **Multiple fringe systems:** Presence of multiple fringe systems that were not aligning caused a variation in the brightness profile of the linear fringes. This affected our determination of Finesse values.

6 Conclusion

In our experiment we successfully measured various quantities, and calculated **finesse** values through different methods, that are tabulated below.

Air spacing [mm] in etalon	$d = 1.62 \pm 0.02$
Wavelength [nm] of green laser	$\lambda_G = 562.92 \pm 15.35$
Free Spectral Range (FSR) [Hz]	$\Delta\nu = 9.26 \times 10^{10} \pm 1.1\%$
Finesse by Airy function fit	$\mathcal{F}_{\text{Airy}} = 1.6367 \pm 0.0188$
Finesse by Lorentzian Peak fits	$\mathcal{F} = 2.4140 \pm 0.0449$
Finesse by Contrast	$\mathcal{F}_C = 4.7208$
Reflectivity Finesse	$\mathcal{F}_{\text{R}} = 2.8074 \pm 0.0136$

References

- Lab manual
- Born, M. and Wolf, E., 2013. *Principles of optics: electromagnetic theory of propagation, interference and diffraction of light*. Elsevier.

Appendix

Table 1: Fringe Number Versus Radius squared for Red Laser

We take the first order radius for m=1. We observe it to be χ_m = 9.005 mm. We subtract its square from the squared fringe radius of every subsequent fringe to obtain the following table:

Fringe Number(n)	χ_{m+n} **(mm)**	$\chi^2_{m+n} - \chi^2_m$(**mm**^{2})
0	9.005	0.000
1	14.490	128.870
2	18.485	260.605
3	21.485	380.515
4	24.475	517.936
5	27.460	672.962
6	29.465	787.096

Table 2: Fringe Number Versus Radius squared for Green Laser

We take the first order radius for m=1. We observe it to be χ_m = 9.015 mm. We subtract its square from the squared fringe radius of every subsequent fringe to obtain the following table:

Fringe Number(n)	χ_{m+n} **(mm)**	$\chi^2_{m+n} - \chi^2_m$(**mm**^{2})
0	9.015	0.000
1	14.475	128.255
2	17.495	224.805
3	20.510	339.390
4	22.995	447.500

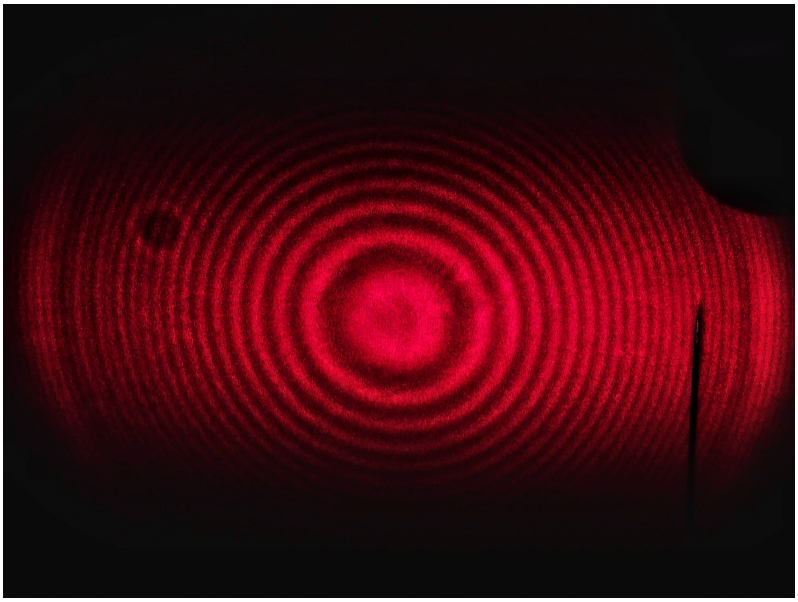


Figure 11: The image of the circular fringe obtained during our experiment with red laser.

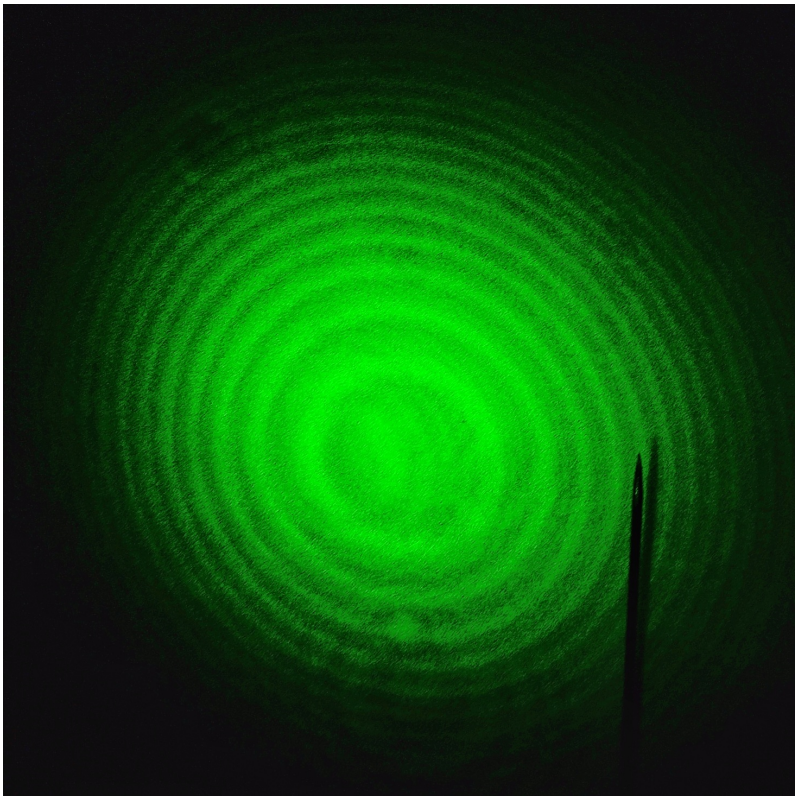


Figure 12: The image of the circular fringe obtained during our experiment with a laser of unknown wavelength.